Self-Association of Model Transmembrane α-Helices Is Modulated by Lipid Structure†

Sanjay Mall, Robert Broadbridge, Ram. P. Sharma, J. Malcolm East, and Anthony G. Lee*

Division of Biochemistry and Molecular Biology, School of Biological Sciences, University of Southampton, Southampton SO16 7PX, U.K.

Received May 24, 2001; Revised Manuscript Received July 26, 2001

ABSTRACT: We have developed a fluorescence quenching method using peptides containing 3,5-dibromotryrosine to measure oligomerization of model transmembrane α-helices in lipid bilayers. Peptides of the type Ac-LysLysGlyLeu$_m$XLeu$_n$LysLysAla-amide where X is tryptophan or 3,5-dibromotyrosine were found to form heterodimers in bilayers of phosphatidylcholine in the liquid-crystalline phase. The free energy of dimer formation changed little with increasing number of Leu residues from 16 to 22 but increased with increasing phospholipid fatty acyl chain length, with a slope of about 0.5 kJ mol^{-1} per fatty acyl chain carbon. Peptides were excluded from lipid in the gel phase, resulting in increased levels of oligomerization. Addition of cholesterol to form the liquid-ordered state led to increased dimerization but without phase separation. The presence of phosphatidylethanolamine had little effect on dimerization.

Transmembrane (TM)[1] α-helices of membrane proteins are often more than simple hydrophobic anchors locating a protein in a membrane. Many membrane proteins containing single TM α-helices associate to form dimers (or larger oligomers) in the membrane, either as stable complexes or as transient species, formed in response to the binding of a suitable ligand. For example, dimerization of the epidermal growth factor receptor family is required for activation (*1*), and interactions between the single TM α-helices of these receptors can be important since mutation of a hydrophobic residue to Glu in the TM α-helix leads to increased dimerization and increased activity, mediated by a hydrogen-bonded interaction between Glu residues in two adjacent helices (*1*). Helix−helix interactions are also important in determining the structure of multispanning membrane proteins. For example, bacteriorhodopsin can be regenerated from two chymotryptic fragments and from a chymotryptic fragment and two separate single-helical domains, showing that interactions between TM α-helices have sufficient specificity to generate the native structure (*2*, *3*). This has led to the description of multispanning proteins as 'collegial' structures in which each TM α-helix first folds as a unit, independent of the rest of the protein, and then pack with the other helices (*4*).

Rees et al. (*5*) have estimated that the residues in the TM domain of the photosynthetic reaction center are as tightly packed as those in a globular protein, implying that van der Waals interactions are central for interhelical packing. An analysis of helix packing in membrane proteins shows that the most common packing angle between adjacent helices is close to 20° (*6*). Helix packing with a crossing angle of about 20° gives a nearly parallel packing of the helices and thus maximizes the area of the interface between the helices. The packing has been described both as ridges into grooves packing of the 3−4 type (*7*) and as knobs into holes packing (*8*). Knobs into holes packing has been found to be particularly useful in describing packing in coiled-coil proteins. In a coiled-coil protein, there may be two, three, or four α-helices in a bundle, with the helices either running in the same (parallel) or running in opposite (antiparallel) directions (*9*). A regular meshing of the side chains in a coiled-coil requires that the side chains occupy equivalent positions around the helix. A small left-handed twist of a regular right-handed α-helix can effectively reduce the number of residues per turn to 3.5 so that the positions of the side chains repeat every 2 turns, equivalent to once every 7 residues. Thus, coiled-coil proteins show a seven-residue or heptad repeat in their sequence; the seven residues in the repeat are given the letters *abcdefg*, and, by convention, residues *a* and *d* are those that provide the contacts at the helix−helix interface. In soluble coiled-coil proteins, helix interactions are driven by hydrophobic interactions of the residues at the *a* and *d* positions; since these are often leucine residues, the structure is referred to as a leucine zipper. Packing of the single TM α-helices of phospholamban into a pentameric structure in a membrane has been proposed to be of the leucine zipper type (*10*).

The free energy of association of two helices in a lipid bilayer, ΔG_a, can be written as

† This work was supported by the BBSRC.

* To whom correspondence should be addressed. Phone: 44 (0) 2380 594222. Fax: 44 (0) 2380 594459. E-mail: agl@soton.ac.uk.

[1] Abbreviations: di(C14:0)PC, dimyristoylphosphatidylcholine; di(C14:1)PC, dimyristoleoylphosphatidylcholine; di(C16:0)PC, dipalmitoylphosphatidylcholine; di(C16:1)PC, dipalmitoleoylphosphatidylcholine; di(C18:1)PC, dioleoylphosphatidylcholine; di(C20:1)PC, dieicosenoylphosphatidylcholine; di(C22:1)PC, dierucoylphosphatidylcholine; di(C24:1)PC, dinervonylphosphatidylcholine; di(C18:1)PE, dioleoylphosphatidylethanolamine; Ac-KKGL$_7$WL$_9$KKA-amide, L$_{16}$; Ac-KKGL$_{10}$WL$_{12}$KKA-amide, L$_{22}$; Ac-KKGL$_7$YL$_9$KKA-amide, Y$_{16}$; Ac-KKGL$_{10}$YL$_{12}$KKA-amide, Y$_{22}$; Ac-KKGL$_7$(dibromotyrosine)-L$_9$KKA-amide, Q$_{16}$; Ac-KKGL$_{10}$(dibromotyrosine)L$_{12}$KKA-amide, Q$_{22}$; FET, fluorescence energy transfer; TM, transmembrane.

10.1021/bi011075y CCC: $20.00
Published on Web 09/22/2001

$$\Delta G_a = \Delta G_{HH} + (n/2)\Delta G_{LL} - n\Delta G_{HL}$$

where ΔG_{HH}, ΔG_{LL}, and ΔG_{HL} are the free energies of helix−helix, lipid−lipid, and helix−lipid interactions, respectively, and it is assumed that formation of a helix−helix pair displaces *n* lipids from around the two helices (*11*, *12*). Dimerization of the helices could be driven by a favorable value for ΔG_{HH}, arising, for example, from salt bridge or hydrogen-bonding interactions between the two helices although, in practice, this turns out to be rare. Good packing at the helix−helix interface with strong van der Waals interactions could also contribute to a favorable value for ΔG_{HH}. Weak interactions between the polar headgroups of the lipids and the helices and poor packing between the lipid fatty acyl chains and the rough surface of the TM α-helices would also drive dimerization since ΔG_{HL} would then be unfavorable compared to ΔG_{HH} and ΔG_{LL}. Any decrease in motional freedom for the lipid fatty acyl chains due to the presence of the relatively rigid TM α-helices will lead to a decrease in chain entropy, also leading to an unfavorable ΔG_{HL}.

Measuring the values of the free energy terms involved in helix interactions in a membrane is difficult. Choma et al. (*13*) used a fluorescence energy transfer (FET) method to study oligomerization of a hydrophobic, Asn-containing peptide in detergent micelles. However, in general FET will not be suitable for measuring oligomerization of TM α-helices in lipid bilayers. FET is 50% efficient at distances typically of about 50 Å (*14*), so that significant energy transfer will be observed over distances of 100 Å or more. FET is therefore only useful for detecting oligomerization in samples where the average distance between unassociated helices is large, as in the presence of high concentrations of detergent micelles. However, in a lipid bilayer at normal lipid:protein ratios, a 100 Å ring around any one helix in the membrane will contain, in addition to any partner helices making up an oligomer, a large number of other helices randomly distributed in the bilayer. We have therefore developed an alternative fluorescence quenching method which is sensitive to just short-range interactions and which can therefore be used to study helix−helix interactions in lipid bilayers. Here we use this method to show that helix−helix interactions in a lipid bilayer are strongly dependent on the physical properties of the lipids making up the bilayer. We synthesized peptides of the type Ac-LysLysGlyLeu$_m$-XLeu$_n$LysLysAla-amide where X is either a Trp group introduced as a fluorescence reporter (L_{m+n}) or a 3,5-dibromotyrosine (Q_{m+n}) group introduced as a fluorescence quencher; values of *m* and *n* were either 7 and 9, respectively (L_{16} and Q_{16}), or 10 and 12, respectively (L_{22} and Q_{22}). The Lys residues serve to anchor the peptide across the membrane; fluorescence emission spectra of the Trp-containing peptides and their quenching by bromine-containing phospholipids confirm that the peptides adopt the expected TM orientation (*15*).

MATERIALS AND METHODS

Dimyristoleoylphosphatidylcholine [di(C14:1)PC], dipalmitoleoylphosphatidylcholine [di(C16:1)PC], dioleoylphosphatidylcholine [di(C18:1)PC], dieicosenoylphosphatidylcholine [di(C20:1)PC], dierucoylphosphatidylcholine [di(C22:1)PC], dinervonylphosphatidylcholine [di(C24:1)PC], and dioleoylphosphatidylethanolamine [di(C18:1)PE] were obtained from Avanti Polar Lipids. Dimyristoylphosphatidylcholine [di(C14:0)PC] and dipalmitoylphosphatidylcholine [di(C16:0)PC] were from Sigma.

Peptides Ac-KKGL$_7$WL$_9$KKA-amide (L_{16}), Ac-KKGL$_{10}$-WL$_{12}$KKA-amide (L_{22}), Ac-KKGL$_7$YL$_9$KKA-amide (Y_{16}), and Ac-KKGL$_{10}$YL$_{12}$KKA-amide (Y_{22}) were synthesized using *t*-Boc chemistry, and purity was confirmed using electrospray mass spectrometry. Tyr-containing peptides were brominated by incubating peptide in methanol with a slight excess of bromine for 30 min, followed by purification on an LH_{20} column, giving the 3,5-dibromotyrosine-containing peptides Ac-KKGL$_7$(dibromotyrosine)L$_9$KKA-amide (Q_{16}) and Ac-KKGL$_{10}$(dibromotyrosine)L$_{12}$KKA-amide (Q_{22}). N^{α}-*t*-Boc-3,5-dibromotyrosine was prepared by bromination of *t*-Boc-tyrosine in the same way. *N*-Hexyl-L-tryptophan *n*-palmitoyl ester was synthesized by reaction of tryptophan with caproic *N*-hydroxysuccinimide ester in dioxane in the presence of sodium hydrogen carbonate, followed by reaction of the product with cetyl alcohol in the presence of 1,3-dicyclohexylcarbodiimide.

Peptides were incorporated into phospholipid bilayers by mixing peptide and lipid at the required molar ratio in methanol. The molar ratio of phospholipid:peptide was maintained above 20:1; full incorporation of peptide into the bilayer requires a phospholipid:peptide molar ratio greater than 15:1 (*16*). Solvent was removed under vacuum, and buffer (20 mM Hepes, pH 7.2, 1 mM EGTA) was added, typically to give 25 μM of the Trp-containing peptide. The sample was placed in a bath sonicator for a few minutes to disperse the lipid−peptide mixture into the buffer, giving a preparation of multilamellar vesicles. Aliquots of the sample were diluted into buffer to give a final concentration of the Trp-containing peptide of 1 μM, and fluorescence intensities were recorded at 25 °C using an SLM-Aminco 8000C fluorometer, with excitation and emission wavelengths of 280 and 330 nm, respectively.

Analysis of Quenching of a Trp-Containing Peptide by a Dibromotyrosine-Containing Peptide. Quenching of fluorescence due to energy transfer from a donor fluorophore to a random distribution of acceptors in a membrane can be described by the equations of Wolber and Hudson (*17*). Quenching of the fluorescence of a Trp-containing TM α-helix by bromine-containing phospholipids has been shown to have a sixth-power dependence on separation distance, consistent with a dipole−dipole, energy transfer quenching mechanism; the value of R_o, the distance at which quenching is 50% efficient, was estimated to be 9.25 Å (*18*). The distance of closest approach between a bromine and a Trp can be estimated to be about 5.5 Å (*19*). When the value for R_o is comparable to the distance of closest approach, the level of quenching becomes dependent on the ratio of these two distances. With an R_o value of 8.2 Å (see below), quenching can be described by the equation (*17*):

$$F_q = F_o[0.6322\exp(-3.1871x_c) + 0.3678\exp(-0.7515x_c)] \quad (1)$$

where F_q and F_o are the fluorescence intensities in the presence and absence of quencher, respectively, and x_c is the concentration of quencher per R_o^2; in calculating R_o^2, the

area per lipid molecule was taken to be 35 Å^2, accounting for the fact that the lipid molecules are organized as a bilayer.

If the Trp-containing peptides (L) and the dibromotyrosine-containing peptides (Q) form dimers in the membrane, the following equilibria need to be considered:

$$L + L \overset{K_1}{\leftrightarrow} L_2$$

$$L + Q \overset{K_2}{\leftrightarrow} LQ$$

$$Q + Q \overset{K_3}{\leftrightarrow} Q_2$$

where K_1−K_3 are association constants. The concentration of free Q, [Q], is given in terms of free L, [L], by the quadratic:

$$[Q] = \frac{-(1 + K_2[L]) + [(1 + K_2[L])^2 + 8K_3[Q]^t]^{1/2}}{4K_3} \quad (2)$$

where $[Q]^t$ is the total concentration of Q. The equations can be solved by the bisection method (*20*) varying the value of [L] until the following equality becomes true:

$$[L] + [LQ] + 2[L_2] - [L]^t = 0 \quad (3)$$

where [LQ], [L_2], and $[L]^t$ are the concentrations of LQ and L_2 and the total concentration of L, respectively. Assuming that the fluorescence of the complex LQ is totally quenched, the observed fluorescence intensity, F_{obs}, is given by

$$F_{obs} = F_q[L]/[L]^t \quad (4)$$

Under conditions where formation of L_2 and Q_2 can be ignored, the concentration of LQ is given by

$$[LQ] = \frac{\left(\frac{1}{K_2} + [Q]^t + [L]^t\right) - \left[\left(\frac{1}{K_2} + [Q]^t + [L]^t\right)^2 - 4[L]^t[Q]^t\right]^{1/2}}{2} \quad (5)$$

and

$$F_{obs} = F_q([L]^t - [LQ])/[L]^t \quad (6)$$

The possibility of trimer formation was also considered:

$$L + L + L \overset{K_1}{\leftrightarrow} L_3$$

$$L + Q + Q \overset{K_2}{\leftrightarrow} LQ_2$$

$$L + L + Q \overset{K_3}{\leftrightarrow} L_2Q$$

$$Q + Q + Q \overset{K_4}{\leftrightarrow} Q_3$$

For the range of parameters used here, the free concentration of Q, [Q], is given by a cubic with one real root given by

$$[Q] = \left[(\sqrt{B^2 - A^3} + |B|)^{1/3} + \frac{A}{(\sqrt{B^2 - A^3} + |B|)^{1/3}}\right] - \frac{a_1}{3} \quad (7)$$

where

$$a_1 = 2K_2[L]/3K_4 \quad (8)$$

$$a_2 = (1 + K_3[L]^2)/3K_4 \quad (9)$$

$$a_3 = -[Q]^t/3K_4 \quad (10)$$

$$A = (a_1^2 - 3a_2)/9 \quad (11)$$

$$B = (2a_1^3 - 9a_1a_2 + 27a_3)/54 \quad (12)$$

Again these equations are solved by the method of bisection, varying the value for [L] until the following equality holds true:

$$[L] + 3[L_3] + 2[L_2Q] + [LQ_2] - [L]^t = 0 \quad (13)$$

The fluorescence intensity in the presence of Q is given by

$$F_{obs} = F_q([L] + 3[L_3])/[L]^t \quad (14)$$

Data were fitted to eq 6 using the Marquardt−Levenberg algorithm in SigmaPlot.

RESULTS

3,5-Dibromotyrosine as a Fluorescence Quencher. Bromine atoms are efficient quenchers of Trp fluorescence (*14*). Quenching of the fluorescence of a hydrophobic analogue of tryptophan, *N*-hexyl-L-tryptophan *n*-palmitoyl ester, by the dibromotyrosine-containing peptide Q_{22} in a bilayer of di(C18:1)PC, as a function of the concentration of Q_{22}, is shown in Figure 1A. Tryptophan analogues of this type have been shown to partition strongly into lipid bilayers and to located in the hydrocarbon core of the bilayer (*21*). Quenching fits to eq 1 with an R_o value of 8.7 ± 0.4 Å, using a value of 5.5 Å for the distance of closest approach between bromine and Trp (*19*). Similarly, quenching of the Trp-containing peptide L_{22} by N^{α}-*t*-Boc-3,5-dibromotyrosine as a function of N^{α}-*t*-Boc-3,5-dibromotyrosine concentration fits to eq 1 with an R_o value of 7.7 ± 0.4 Å (Figure 1A). Thus, in subsequent experiments nonspecific quenching of Trp fluorescence was accounted for by using eq 1 with an average R_o value of 8.2 Å. It is worth noting that the value of R_o is not important as such in the following experiments: what is important is that eq 1 accounts accurately for the small nonspecific quenching effects that are seen, as shown by the goodness of fit for the nonspecific quenching data in Figure 1A to eq 1.

TM α-Helices Form Dimers in the Lipid Bilayer. Quenching of the fluorescence of L_{22} by Q_{22} in lipid bilayers is more efficient than quenching by N^{α}-*t*-Boc-3,5-dibromotyrosine, and the quenching efficiency increases with increasing phospholipid chain length, indicative of phospholipid-dependent oligomerization of L_{22} and Q_{22} (Figure 1A). The level of quenching of L_{22} by Q_{22} in di(C18:1)PC is unchanged on changing the mole fraction of L_{22} from 0.004 to 0.001 (Figure 2A). Oligomerization of Leu-rich polypeptides can give coiled-coil structures of dimers, trimers, or tetramers (*22*). Quenching of L_{22} fluorescence could therefore follow from formation of a mixed dimer $L_{22}Q_{22}$, mixed trimers $L_{22}Q_{22}Q_{22}$ or $L_{22}L_{22}Q_{22}$, and so on. To distinguish between

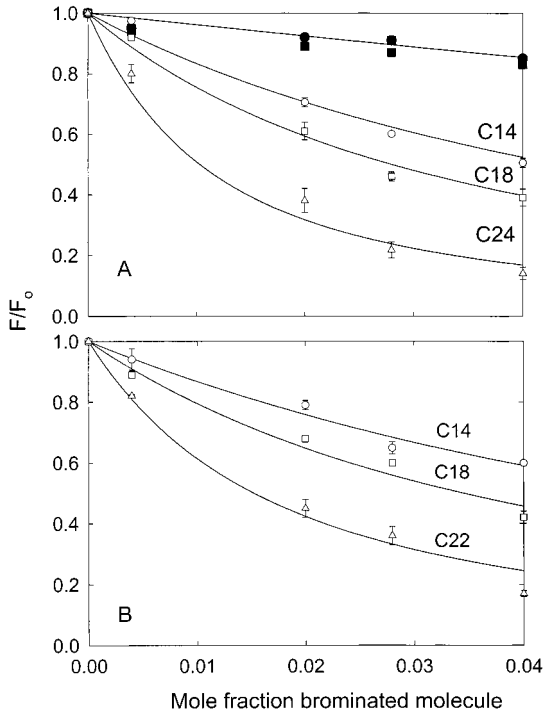

FIGURE 1: Quenching of Trp fluorescence by 3,5-dibromotyrosine. (A) The filled symbols show the quenching (F/F_o) of L_{22} by N^{α}-*t*-Boc-3,5-dibromotyrosine (●) and *N*-hexyl-L-tryptophan *n*-palmitoyl ester by Q_{22} (■). The line shows a fit to the equations of Wolber and Hudson (*17*) with a distance of closest approach of 5.5 Å and a distance R_o of 7.7 ± 0.4 Å. The open symbols show the quenching of L_{22} by the given mole fraction of Q_{22} in bilayers of (○) di(C14:1)PC, (□) di(C18:1)PC, and (△) di(C24:1)PC. (B) Quenching of L_{16} by the given mole fraction of Q_{16} in bilayers of (○) di(C14:1)PC, (□) di(C18:1)PC, and (△) di(C22:1)PC. The mole fractions of L_{22} and L_{16} in the lipid bilayer were 0.004. The solid lines show fits to a dimer model, with the association constants given in Table 1.

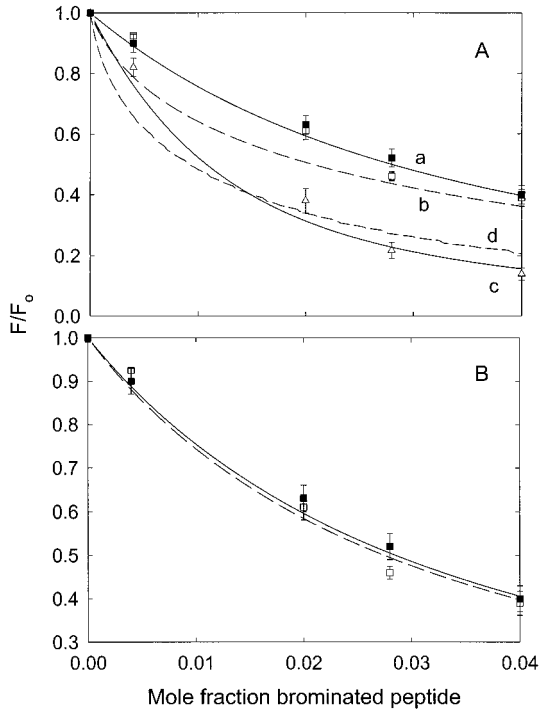

FIGURE 2: Simulations of quenching for the dimer model. Shown are data for quenching of L_{22} by Q_{22} in di(C18:1)PC (□,■) or di(C24:1)PC (△), at mole fractions of L_{22} of 0.004 (□,△) and 0.001 (■). In (A), curves a and b are simulations of the data in di(C18:1)PC, and curves c and d are simulations of the data in di(C24:1)PC. Values for the association constants (mol fraction^{-1}) used in the simulations are as follows: (a) $K_1 = K_2 = 35$, $K_3 = 0$; (b) $K_1 = K_2 = K_3 = 300$; (c) $K_1 = K_2 = 150$, $K_3 = 0$; (d) $K_1 = K_2 = K_3 = 4 \times 10^5$. In (B), the lines show simulations with a mole fraction of L_{22} of 0.004: solid line, simulation (a) from above ($K_1 = K_2 = 35$, $K_3 = 0$); broken line, a simulation with $K_1 = 0$, $K_2 = 30$, $K_3 = 0$. A simulation with a mole fraction of L_{22} of 0.001 and $K_1 = 0$, $K_2 = 30$, $K_3 = 0$ is almost identical to the broken line.

dimer and higher oligomer formation, the experimental data were compared with simulations calculated according to the equations given under Materials and Methods. Simulations of the data using the dimer model (eq 2) for quenching of L_{22} by Q_{22} in di(C18:1)PC or di(C24:1)PC are very poor if the association constants K_1, K_2, and K_3 for formation of $L_{22}L_{22}$, $L_{22}Q_{22}$, and $Q_{22}Q_{22}$, respectively, are equal (Figure 2A, broken lines, with values for the association constants chosen to match the maximum quenching observed at a mole fraction of Q_{22} of 0.04). However, if formation of the $Q_{22}Q_{22}$ dimer is very weak ($K_3 = 0$), good agreement with the experimental data can be obtained with $K_1 = K_2 = 35$ mol fraction^{-1} in di(C18:1)PC and $K_1 = K_2 = 300$ mol fraction^{-1} in di(C24:1)PC (Figure 2A, solid lines). Homodimer formation between Q_{22} molecules could be weak because of steric packing problems with the bulky 3,5-dibromotyrosine. Equally good agreement with the experimental data can be obtained assuming that only the $L_{22}Q_{22}$ dimer is formed ($K_1 = K_3 = 0$) with a slightly decreased value for K_2; for example, the data in di(C18:1)PC fit well with $K_1 = K_3 = 0$ and $K_2 = 30$ mol fraction^{-1} (Figure 2B, solid line). Homodimer formation by L_{22} molecules has only a small effect on the simulations because the concentrations of Q_{22} at which high levels of quenching are seen are much higher than the concentrations of L_{22}, so that concentration of any $L_{22}L_{22}$ formed will be low compared to the concentration of $L_{22}Q_{22}$.

For the trimer model (eq 7), reasonable agreement with the experimental data in di(C18:1)PC can be obtained with $K_1 = K_2 = K_3 = K_4 = 8000$ mol fraction^{-2} (Figure 3, curve c). However, good agreement cannot be obtained with the experimental data in di(24:1)PC; matching the quenching observed in di(C24:1)PC at high mole fractions of Q_{22} requires a large value for the association constants ($K_1 = K_2 = K_3 = K_4 = 4 \times 10^5$ mol fraction^{-2}), but then poor agreement is obtained with the experimental data at low mole fractions of Q_{22} (Figure 3, curve e). Reasonable agreement with the experimental data in di(C18:1)PC can also be obtained if it is assumed that formation of $Q_{22}Q_{22}Q_{22}$ and $L_{22}Q_{22}Q_{22}$ trimers is very weak ($K_2 = K_4 = 0$) (Figure 3, curve b). However, poor agreement is again observed in di(C24:1)-PC; if values of K_1 and K_3 are chosen to match the experimental data at high mole fractions of Q_{22}, then agreement is poor at low mole fractions of Q_{22} (Figure 3, curve d). Further, if it is assumed that quenching depends on the proportion of L_{22} present as the quenched trimeric specifies $L_{22}L_{22}Q_{22}$, then the level of quenching will be dependent on the concentration of L_{22} in the membrane, and the level of quenching would be expected to decrease with a decrease in the mole fraction of L_{22} in the membrane from 0.004 to 0.001 (Figure 3, curves a and c), and this is not observed experimentally. In fact, if quenching depends on formation of any species containing more than one molecule of L_{22}, the observed level of quenching will be strongly dependent on the concentration

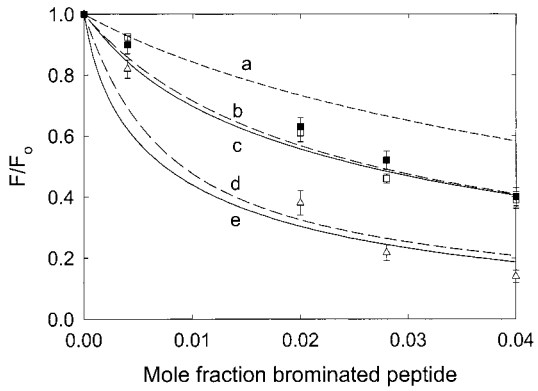

FIGURE 3: Simulations of quenching for the trimer model. Shown are data for quenching of L_{22} by Q_{22} in di(C18:1)PC (□,■) or di(C24:1)PC (△), at mole fractions of L_{22} of 0.004 (□,△) and 0.001 (■). Solid lines c and e and broken lines b and d are simulations of the data in di(C18:1)PC and di(C24:1)PC, respectively, with a mole fraction of L_{22} of 0.004, with values for the association constants (mol fraction^{-1}) as follows: (c) $K_1 = K_2 = K_3 = K_4 = 8000$; (e) $K_1 = K_2 = K_3 = K_4 = 4 \times 10^5$; (b) $K_2 = K_4 = 0$ and $K_1 = K_3 = 8000$; (d) $K_2 = K_4 = 0$ and $K_1 = K_3 = 50\,000$. Dashed line a is a simulation for a mole fraction of L_{22} of 0.001 in di(C18:1)PC with $K_2 = K_4 = 0$ and $K_1 = K_3 = 8000$.

Table 1: Association Constants for Dimer Formation in Phosphatidylcholines at 25 °C

	K_2 (mol fraction^{-1})	
fatty acyl chain length	$L_{16} + Q_{16}$	$L_{22} + Q_{22}$
C14	10.4 ± 1.5	15.5 ± 1.5
C16	14.1 ± 2.2	19.8 ± 1.2
C18	21.8 ± 3.7	29.2 ± 3.3
C20	49.1 ± 7.4	33.0 ± 3.0
C22	65.4 ± 19.5	41.7 ± 2.3
C24	−	97.3 ± 12.0

of L_{22} in the bilayer. Since this is not observed, it is possible to reject formation of any oligomeric species higher than a dimer. Thus, the experimental data are consistent with formation of the simple heterodimer $L_{22}Q_{22}$, allowing the experimental data to be fitted directly to eq 5.

Effect of Phospholipid Chain Length on Dimerization. As shown in Figure 1A, quenching of L_{22} fluorescence by Q_{22} fits to dimer formation (eq 5) with association constants increasing from 15.5 ± 1.5 mol fraction^{-1} in di(C14:1)PC to 97.3 ± 12.0 mol fraction^{-1} in di(C24:1)PC (Table 1). Quenching of L_{16} fluorescence by Q_{16} could only be studied in the chain length range C14−C22 since L_{16} does not incorporate into bilayers of di(C24:1)PC (*16*). Within this range, quenching of L_{16} fluorescence by Q_{16} is very similar to that seen with L_{22} and Q_{22} (Figure 1B; Table 1). Unitary free energies for dimer formation increase linearly with increasing number of carbon atoms in the fatty acyl chains with slopes of 0.45 ± 0.04 kJ mol^{-1} per carbon atom and 0.63 ± 0.06 kJ mol^{-1} per carbon atom for $L_{22}Q_{22}$ and $L_{16}Q_{16}$, respectively (Figure 4).

Effects of Gel-Phase Lipid. Studies of the quenching of L_{16} and L_{22} fluorescence by dibromostearoylphosphatidylcholine in mixtures with di(C16:0)PC show that the peptides are excluded from gel-phase lipid to form domains enriched in peptide (*15*). The fluorescence intensity of a 1:5 mixture of L_{22} and Q_{22} in di(C16:0)PC decreases markedly as the temperature decreases below 41 °C (Figure 5), corresponding to the temperature of the gel- to liquid-crystalline phase

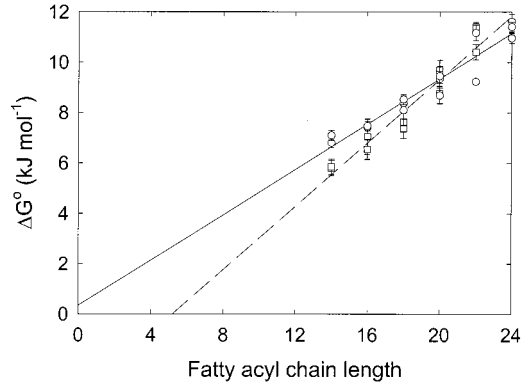

FIGURE 4: Unitary free energy changes for dimerization of TM α-helices in bilayers of phosphatidylcholine. Values of the unitary free energy change for heterodimerization are plotted as a function of fatty acyl chain length for $L_{22}Q_{22}$ (○) and $L_{16}Q_{16}$ (□) in bilayers of phosphatidylcholines containing monounsaturated fatty acyl chains. The solid and broken lines show linear least-squares fits to the data for $L_{22}Q_{22}$ and $L_{16}Q_{16}$, respectively.

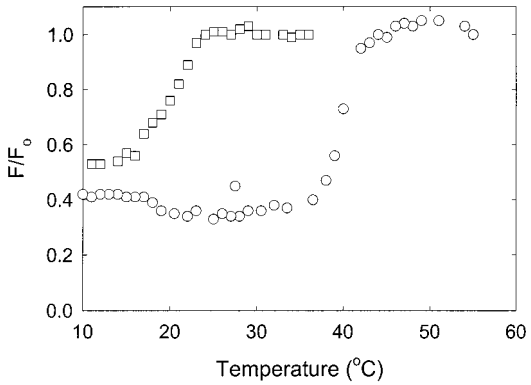

FIGURE 5: Effect of temperature on fluorescence quenching of L_{22} by Q_{22}. The relative fluorescence intensity F/F_o for L_{22} is given for bilayers containing L_{22} and Q_{22} in di(C16:0)PC (○) or di(C14:0)PC (□) at L_{22}:lipid and Q_{22}:lipid molar ratios of 1:250 and 1:50, respectively, at the given temperatures (°C). Intensities are expressed relative to those observed at 55 °C for di(C16:0)PC or at 36 °C for di(C14:0)PC.

transition of di(C16:0)PC (42 °C). A similar result is seen in bilayers of di(C14:0)PC with a decrease in fluorescence intensity below 22 °C (Figure 5), corresponding to the phase transition temperature at 24 °C. These effects of temperature were fully reversible. No significant change in fluorescence intensity was seen at the temperature of the phase transition for L_{22} alone in either di(C14:0)PC or di(C16:0)PC.

The decreases in fluorescence intensities for the L_{22}/Q_{22} mixtures on going below the phase transition temperature of the phospholipid are consistent with exclusion of peptides from gel-phase lipid, forming domains enriched in L_{22} and Q_{22} where oligomer formation will be favored by the high local concentration of peptide. The sharpness of the change in fluorescence intensity with temperature is also consistent with exclusion of peptide by gel-phase lipid since formation of a homogeneous mixture of peptide and lipid would lead to a broad phase transition (*23*).

Quenching of L_{22} fluorescence by Q_{22} in mixtures of di(C16:0)PC and di(C18:1)PC at a temperature (25 °C) where both liquid-crystalline and gel-phase domains will be present (*24*) is independent of di(C16:0)PC content up to 40 mol % but then increases linearly with increasing di(C16:0)PC content (Figure 6). This is consistent with the phase diagram

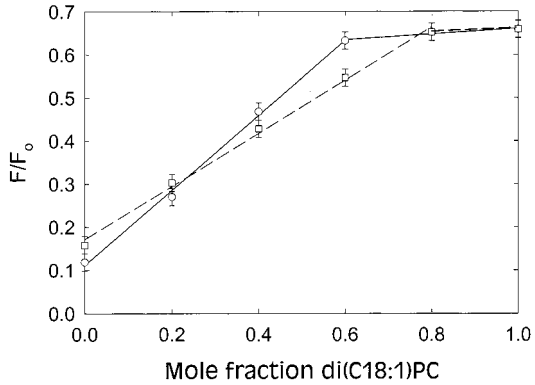

FIGURE 6: Effect of gel-phase lipid. F/F_o values are given for bilayers containing L_{22} and Q_{22} in di(C18:1)PC/di(C16:0)PC mixtures (○) and L_{16} and Q_{16} in di(C18:1)PC/sphingomyelin mixtures (□), at the given mole fractions of di(C18:1)PC. Fluorescence intensities are expressed relative to that for L_{16} or L_{22} alone in di(C18:1)PC.

for the di(C16:0)PC−di(C18:1)PC system which shows separation of a gel-phase domain at about 40 mol % di(C16:0)-PC at 25 °C (*24*). A very similar result is observed for quenching of L_{16} fluorescence by Q_{16} in mixtures of bovine brain sphingomyelin and di(C18:1)PC, where quenching increases linearly with increasing content of sphingomyelin beyond 20 mol % (Figure 6). The high transition temperature for bovine brain sphingomyelin [ca. 35 °C, (*25*)] means that in mixtures with a liquid-crystalline phospholipid, separate domains will form highly enriched in phospholipid and sphingomyelin, respectively (*26*), and peptides are excluded from gel-phase sphingomyelin (*15*).

Effects of Cholesterol. Addition of cholesterol to a phospholipid bilayer in the liquid-crystalline phase results in an increase in order for the fatty acyl chains with formation of a liquid-ordered phase (*27*). Unlike formation of the gel state, formation of the liquid-ordered state does not lead to separation of peptide- and lipid-enriched phases since it has been shown that dibromocholesterol quenches the fluorescence of L_{22} in lipid bilayers (*15, 28*), showing that cholesterol is in close contact with L_{22} in these bilayers. Addition of cholesterol to di(C18:1)PC leads to increased quenching of L_{22} by Q_{22} (Figure 7). Addition of cholesterol to L_{22} alone in di(C18:1)PC had no significant effect on fluorescence intensity (data not shown). Fluorescence quenching of L_{22} by Q_{22} in a 1:1 mixture of di(C18:1)PC and cholesterol is consistent with dimer formation described by an association constant of 186 ± 23 mol fraction^{-1} (Figure 8). The linear dependence of fluorescence intensity on the molar ratio of cholesterol to di(C18:1)PC is consistent with a model in which separate domains of cholesterol and a 1:1 'complex' of cholesterol and di(C18:1)PC are formed, with the peptide partitioning equally between these domains.

Effects of Di(C18:1)PE. Attempts to incorporate peptides into bilayers of di(C18:1)PE failed due to the formation of granular, nonbilayer structures. However, peptides could be incorporated at the required mole fractions into bilayers containing a 1:1 molar ratio of di(C18:1)PE and di(C18:1)-PC. Quenching of L_{22} by Q_{22} in the di(C18:1)PE/di(C18:1)-PC mixture fitted to a dimer model with an association constant of 25.5 ± 3.1 mol fraction^{-1} at 25 °C (Figure 9), comparable to the value in di(C18:1)PC at 25 °C (Table 1). The value of the association constant decreases slightly with increasing temperature, having values of 32.9 ± 1.1 and 16.9 ± 1.2 mol fraction^{-1} at 15 and 40 °C, respectively (Figure 9).

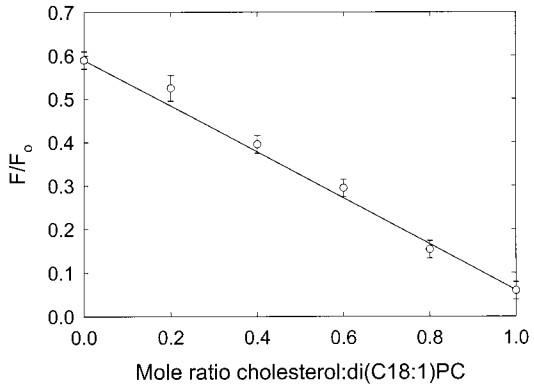

FIGURE 7: Effect of cholesterol on quenching of L_{22} by Q_{22}. F/F_o values (○) are given for bilayers containing L_{22} and Q_{22} in di(C18:1)PC at L_{22}:di(C18:1)PC and Q_{22}:di(C18:1)PC molar ratios of 1:250 and 1:50, respectively, at the given cholesterol:di-(C18:1)PC molar ratios. Fluorescence intensities are expressed relative to that for L_{22} alone in di(C18:1)PC. The solid line shows the calculated result for equal partition of peptide between separate domains of di(C18:1)PC and a 1:1 'complex' of di(C18:1)PC and cholesterol, with association constants for dimer formation of 29 and 186 in di(C18:1)PC and in the 1:1 di(C18:1)PC−cholesterol complex, respectively.

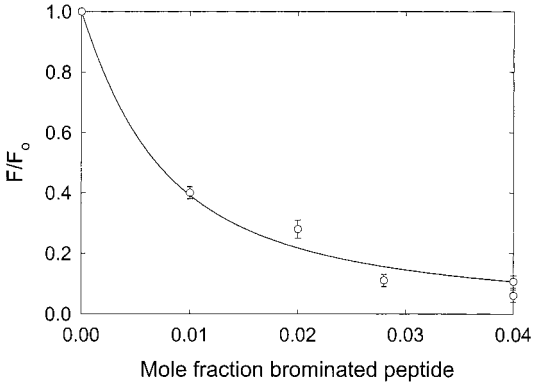

FIGURE 8: Quenching of the fluorescence of L_{22} by Q_{22} in bilayers of a 1:1 mixture of cholesterol and di(C18:1)PC. The experimental points show the quenching of the fluorescence of L_{22} present at a mole fraction of 0.004 with respect to di(C18:1)PC by Q_{22} at the given mole fraction. The solid line shows the best fit to the dimer model, giving an association constant of 186 ± 23 mol fraction^{-1}.

DISCUSSION

TM α-helices have been described as individually stable, self-folding entities (*29*). Packing of TM α-helices in a lipid bilayer will depend on the relative strengths of the helix−helix, helix−lipid, and lipid−lipid interaction energies. Rees et al. (*5*) have estimated that residues in the TM domains of membrane proteins are as tightly packed as those in a globular protein, implying that van der Waals interactions are central for helix packing. An analysis of helix packing in membrane proteins shows that the most common packing angle between adjacent helices is close to 20°, giving a nearly parallel packing of the helices, thus maximizing the area of the interface between the helices (*6*). Packing will therefore be similar to that in a coiled-coil protein such as the yeast transcription factor GCN4 (*22*), and, indeed, the structure of GCN4 has been used in developing models for TM α-helical bundles (*13, 29*).

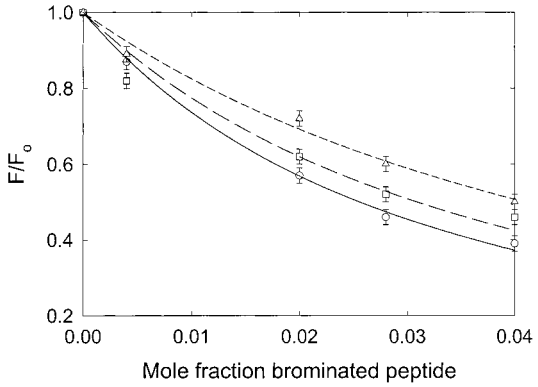

FIGURE 9: Quenching of the fluorescence of L_{22} by Q_{22} in bilayers of a 1:1 mixture of di(C18:1)PE and di(C18:1)PC. The experimental points show the quenching of the fluorescence of L_{22} present at a mole fraction of 0.004 by Q_{22} at the given mole fraction, at temperatures (°C) of (○) 15, (□) 25, and (△) 40. The solid, broken, and dotted lines show the best fit to the dimer model, with the association constants given in the text.

In GCN4, helix−helix interactions are mediated by leucine zipper sequences with a heptad repeat in which hydrophobic residues at the *a* and *d* positions of the repeat pack tightly as 'knobs into holes' at the helix−helix interface (*22*). Oligomerization of soluble coiled-coil proteins is driven by packing of hydrophobic residues at the interface, but hydrophobic interactions cannot be important in oligomerization of TM α-helices since hydrophobic interactions are already accounted for in insertion of the helices into the lipid bilayer. However, the tight packing observed at the helix−helix interface for α-helices containing a leucine zipper could favor oligomerization in a membrane. Indeed, Gurezka et al. (*30*) reported that oligomerization of the ToxR protein of *Vibrio cholerae* could be driven by TM α-helices containing just 16 Leu residues or by helices with Leu residues at the *ga* and *de* positions of a heptad repeat with the other position occupied by Ala, but not by helices containing just 16 Ala residues. In contrast, Zhou et al. (*29*) reported that a chimera of staphylococcal nuclease with a TM α-helix of 22 Leu residues did not form stable dimers in SDS and that any dimer formation by the ToxR protein with a TM α-helix containing 22 Leu residues was very weak.

The results presented here show that oligomerization of peptides in a lipid bilayer can be detected by observing the quenching of the fluorescence of a Trp-containing peptide by a dibromotyrosine-containing peptide. The dependence of quenching on the concentrations of the Trp-containing and dibromotyrosine-containing peptides is consistent with dimer formation in the membrane, rather than with trimer or higher oligomer formation. The absolute values for the association constants and free energies for heterodimer formation between the Trp-containing and dibromotyrosine-containing peptides are likely to be affected by the presence of the Trp and 3,5-dibromotyrosine groups, but the similar values observed for peptides containing 16 or 22 residues (Figure 4; Table 1) suggest that a major contribution to the free energy of dimerization comes from interaction with the lipid. This is also consistent with the marked increase in free energy of dimerization with increasing chain length (Figure 4). In di(C18:1)PC, the free energy of dimerization is 8.4 kJ mol^{-1} (Figure 4). As described by White and Wimley (*11*), the free energy of dimerization can be compared to the free energy cost of creating a void equivalent to a methyl group in the hydrophobic core of a soluble protein, which is about 6.7 kJ mol^{-1}. The free energy change favoring helix dimer formation in di(C18:1)PC is therefore that expected if helix−helix packing were more efficient than helix−lipid packing by an amount equivalent to the volume of about one methyl group. A comparison can also be made with the entropy change corresponding to disordering of the lipid fatty acyl chains at the gel- to liquid-crystalline-phase transition (*31*), which corresponds to a free energy change of ca. 2.9 kJ mol^{-1} per carbon atom. The free energy for dimer formation increases with increasing chain length by about 0.5 kJ mol^{-1} per carbon atom (Figure 4). Thus, a relatively small increase in chain order caused by the presence of the peptide could make a significant contribution to the free energy for oligomerization of TM α-helices.

A chain-length dependence of the energy of helix−helix packing could be part of the explanation for the chain-length dependence of the activities of some membrane proteins. For example, the ATPase activity of the Ca^{2+}-ATPase of sarcoplasmic reticulum is greatest in di(C18:1)PC, with lower activities in phosphatidylcholines with shorter or longer fatty acyl chains (*32*). The crystal structure of the Ca^{2+}-ATPase shows that the 10 TM α-helices are only linked by small loops on the lumenal side of the membrane (*33*) and transport of Ca^{2+} across the membrane must involve changes in the packing of the helices (*34*). Changes in the energies of helix−helix interactions as a result of changing phospholipid chain length could therefore have significant effects on the packing of the 10 TM α-helices and so affect activity.

The results presented here also show that the physical phase of the phospholipids in the membrane has a marked effect on oligomerization of TM α-helices. In lipid bilayers containing domains of liquid-crystalline and gel-phase lipid, TM α-helices partition preferentially into regions of liquid-crystalline lipid (*15*). In bilayers containing predominantly gel-phase lipid, TM α-helices have been shown to form ordered line-like aggregates surrounded by lipids in a liquid-crystalline-like state (*35*). The presence of gel-phase lipid will therefore increase the local concentration of peptide in the bilayer and thus lead to an increase in oligomer formation, as observed (Figures 5 and 6). The plasma membranes of eukaryotic cells often contain lipids such as the sphingolipids which, in isolation, will be in the gel phase at physiological temperatures, and the presence of sphingolipids leads to increased oligomerization of the TM α-helices (Figure 6). However, strong association between sphingolipids and cholesterol, forming a 1:1 'complex', means that, in the plasma membrane, sphingolipids will be present as 'rafts' in a liquid-ordered state (*36*). TM α-helices are not excluded from liquid-ordered lipid (*15*). However, in liquid-ordered lipid, helix dimerization is stronger than in liquid-crystalline lipid (Figure 7), with a free energy for heterodimerization of 13.1 kJ mol^{-1} for L_{22} and Q_{22} in a 1:1 mixture of di(C18:1)PC and cholesterol, compared to 8.4 kJ mol^{-1} in di(C18:1)PC alone. In part the effect of cholesterol will follow from an increase in the effective chain length of the phospholipid. Studies of relative lipid−peptide binding constants suggest that the effect of a 1:1 molar ratio of cholesterol to phosphatidylcholine is to increase the effective lipid chain length by about four carbons (*16*). Since the free energy change for dimerization in di(C22:1)PC is about 10 kJ mol^{-1}

(Figure 4), effects of cholesterol are, in fact, more than expected simply from a change in effective chain length. It is possible that the cost of formation of voids at the lipid−protein interface in the liquid-ordered state is higher than in the liquid-crystalline state, because of the increased packing density in the liquid-ordered state, and that this will also contribute to favorable dimerization of the helices. These results suggest that the presence of cholesterol in a membrane could have significant effects on the packing of TM α-helices and so on membrane protein function.

We have also investigated the possible effects of phosphatidylethanolamines on helix−helix interactions. It has been suggested that the presence in a bilayer of phospholipids such as phosphatidylethanolamines which prefer the hexagonal H_{II} phase will result in curvature frustration in the bilayer because the phosphatidylethanolamine will make unequal contributions to the headgroup and chain areas (*37*). This curvature frustration would result in increased surface free energy (increased surface tension) owing to increased water contact with the hydrocarbon core of the bilayer. The increased surface tension would, in turn, result in an increased lateral compression in the acyl chain region, and it has been suggested that this could modulate the function of some membrane proteins (*37*). It has been shown, for example, that the presence of lipids able to form a hexagonal H_{II} phase is required to produce the metarhodopsin II to metarhodopsin I ratio found for rhodopsin in the retinal rod membrane (*38*). In contrast, the presence of di(C18:1)PE has little effect on the activity of the Ca^{2+}-ATPase of sarcoplasmic reticulum, as long as the lipids remain in a bilayer structure (*39*).

The presence of 50 mol % di(C18:1)PE has no significant effect on the quenching of L_{22} fluorescence by Q_{22} at 25 °C, the association constant for dimer formation (25.5 ± 3.1 mol fraction^{-1}) being equal to that in di(C18:1)PC alone (Figure 9). The temperature of the bilayer/hexagonal H_{II} phase transition for di(C18:1)PE is 9 °C (*40*). Quenching of L_{22} fluorescence by Q_{22} varies only slightly with temperature, the value of the association constant decreasing from 32.9 ± 1.1 mol fraction^{-1} at 15 °C to 16.9 ± 1.2 mol fraction^{-1} at 40 °C (Figure 9). Thus, the presence of phosphatidylethanolamine, even at temperatures where in isolation it will adopt a hexagonal H_{II} structure, has little if any effect on helix−helix interactions.

In conclusion, leucine-rich TM α-helices have a strong tendency to dimerize in lipid bilayers. The free energy of dimer formation by a poly-Leu helix in di(C18:1)PC is about half the free energy of association of a preformed six TM α-helix fragment of bacteriorhodopsin with the missing TM α-helix, which has been estimated to be about 15 kJ mol^{-1} (*11*). Interaction between TM α-helices could be made specific by the presence of suitable hydrogen-bonding partners in the helices (*13*, *29*) or by the presence of Glu-containing motifs that will allow particularly close packing at the helix−helix interface (*41*).

REFERENCES

1. Smith, S. O., Smith, C. S., and Bormann, B. J. (1996) *Nat. Struct. Biol. 3,* 252−258.
2. Popot, J. L., Gerchman, S. E., and Engelman, D. M. (1987) *J. Mol. Biol. 198,* 655−676.
3. Kahn, T. W., and Engelman, D. M. (1992) *Biochemistry 31,* 6144−6151.
4. Popot, J. L., de Vitry, C., and Atteia, A. (1994) in *Membrane Protein Structure* (White, S. H., Ed.) pp 41−96, OUP, New York.
5. Rees, D. C., Komiya, H., Yeates, T. O., Allen, J. P., and Feher, G. (1989) *Annu. Rev. Biochem. 58,* 607−633.
6. Bowie, J. U. (1997) *J. Mol. Biol. 272,* 780−789.
7. Rees, D. C., Chirino, A. J., Kim, K. H., and Komiya, H. (1994) in *Membrane Protein Structure* (White, S. H., Ed.) pp 3−26, OUP, New York.
8. Langosch, D., and Heringa, J. (1998) *Proteins: Struct., Funct., Genet. 31,* 150−159.
9. Lupas, A. (1996) *Trends Biochem. Sci. 21,* 375−382.
10. Torres, J., Adams, P. D., and Arkin, I. T. (2000) *J. Mol. Biol. 300,* 677−685.
11. White, S. H., and Wimley, W. C. (2000) *Annu. Rev. Biophys. Biomol. Struct. 28,* 319−365.
12. Lemmon, M. A., and Engelman, D. M. (1994) *Q. Rev. Biophys. 27,* 157−218.
13. Choma, C., Gratkowski, H., Lear, J. D., and DeGrado, W. F. (2000) *Nat. Struct. Biol. 7,* 161−166.
14. Lakowicz, J. R. (1999) *Principles of Fluorescence Spectroscopy*, Plenum Press, New York.
15. Mall, S., Broadbridge, R., Sharma, R. P., Lee, A. G., and East, J. M. (2000) *Biochemistry 39,* 2071−2078.
16. Webb, R. J., East, J. M., Sharma, R. P., and Lee, A. G. (1998) *Biochemistry 37,* 673−679.
17. Wolber, P. K., and Hudson, B. S. (1979) *Biophys. J. 28,* 197−210.
18. Bolen, E. J., and Holloway, P. W. (1990) *Biochemistry 29,* 9638−9643.
19. Zelent, B., Kusba, J., Gryczynski, I., Johnson, M. L., and Lakowicz, J. R. (1998) *Biophys. Chem. 73,* 53−75.
20. Press, W. H., Flannery, B. P., Teukolsky, S. A., and Vetterling, W. T. (1986) *Numerical Recipes*, CUP, Cambridge.
21. Froud, R. J., East, J. M., Rooney, E. K., and Lee, A. G. (1986) *Biochemistry 25,* 7535−7544.
22. Harbury, P. B., Zhang, T., Kim, P. S., and Alber, T. (1993) *Science 262,* 1401−1407.
23. Lee, A. G. (1977) *Biochim. Biophys. Acta 472,* 285−344.
24. East, J. M., and Lee, A. G. (1982) *Biochemistry 21,* 4144−4151.
25. Untracht, S. M., and Shipley, G. G. (1977) *J. Biol. Chem. 252,* 4449−4457.
26. Bar, L. K., Barenholz, Y., and Thompson, T. E. (1997) *Biochemistry 36,* 2507−2516.
27. Finegold, L. (1993) *Cholesterol in membrane models*, CRC Press, Boca Raton, FL.
28. Mall, S., Sharma, R. P., East, J. M., and Lee, A. G. (1998) *Faraday Discuss. 111,* 127−136.
29. Zhou, F. X., Cocco, M. J., Russ, W. P., Brunger, A. T., and Engelman, D. M. (2000) *Nat. Struct. Biol. 7,* 154−160.
30. Gurezka, R., Laage, R., Brosig, B., and Langosch, D. (1999) *J. Biol. Chem. 274,* 9265−9270.
31. Marsh, D. (1990) *CRC Handbook of Lipid Bilayers*, CRC Press, Boca Raton, FL.
32. Lee, A. G. (1998) *Biochim. Biophys. Acta 1376,* 381−390.
33. Toyoshima, C., Nakasako, M., Nomura, H., and Ogawa, H. (2000) *Nature 405,* 647−655.
34. Lee, A. G., and East, J. M. (2001) *Biochem. J. 356,* 665−683.
35. Rinia, H. A., Kik, R. A., Demel, R. A., Snel, M. M. E., Killian, J. A., van der Eerden, J. P. J. M., and de Kruijff, B. (2000) *Biochemistry 39,* 5852−5858.
36. Simons, K., and Ikonen, E. (1997) *Nature 387,* 569−572.
37. Gruner, S. M. (1985) *Proc. Natl. Acad. Sci. U.S.A. 82,* 3665−3669.
38. Brown, M. F. (1994) *Chem. Phys. Lipids 73,* 159−180.
39. Starling, A. P., Dalton, K. A., East, J. M., Oliver, S., and Lee, A. G. (1996) *Biochem. J. 320,* 309−314.
40. Cullis, P. R., and de Kruijff, B. (1979) *Biochim. Biophys. Acta 559,* 399−420.
41. Lemmon, M. A., Treutlein, H. R., Adams, P. D., Brunger, A. T., and Engelman, D. M. (1994) *Nat. Struct. Biol. 1,* 157−163.

BI011075Y